# Sources and Variability of Greenhouse Gases over Greece

Aikaterini Bougiatioti, Nikos Gialesakis, Yannis Sarafidis, Maria I Gini, Marios Mermigkas, Panayiotis Kalkavouras, Sebastian Mirasgedis, Michel Ramonet, Clement Narbaud, Morgan Lopez, et al.

atmosphere

MDPI

*Article*

# Sources and Variability of Greenhouse Gases over Greece

**Aikaterini Bougiatioti [1,*], Nikos Gialesakis [2,3], Yannis Sarafidis [1], Maria I. Gini [4], Marios Mermigkas [5], Panayiotis Kalkavouras [1,6], Sebastian Mirasgedis [1], Michel Ramonet [7], Clement Narbaud [7], Morgan Lopez [7], Dimitris Balis [5], Konstantinos Eleftheriadis [4], Maria Kanakidou [2,3,8] and Nikolaos Mihalopoulos [1]**

1 Institute for Environmental Research and Sustainable Development, National Observatory of Athens, 15236 Athens, Greece; pkalkavouras@noa.gr (P.K.); seba@noa.gr (S.M.)
2 Environmental Chemical Processes Laboratory, Department of Chemistry, University of Crete, 70013 Heraklion, Greece
3 Institute of Environmental Physics, University of Bremen, 28359 Bremen, Germany
4 Environmental Radioactivity and Aerosol Technology for Atmospheric and Climate Impact Laboratory, NCSR "Demokritos", 15310 Athens, Greece; elefther@ipta.demokritos.gr (K.E.)
5 Laboratory of Atmospheric Physics, Department of Physics, Aristotle University of Thessaloniki, 54124 Thessaloniki, Greece; mmermigk@physics.auth.gr (M.M.)
6 Department of Environment, University of the Aegean, 81100 Mytilene, Greece
7 Laboratoire des Sciences du Climat et de l'Environnement (LSCE), IPSL, CEA-CNRS UVSQ, University Paris-Saclay, Orme des Merisiers, 91191 Gif-sur-Yvette, France; michel.ramonet@lsce.ipsl.fr (M.R.); clement.narbaud@lsce.ipsl.fr (C.N.); morgan.lopez@lsce.ipsl.fr (M.L.)
8 Center for the Study of Air Quality & Climate Change (CSTACC), Institute of Chemical Engineering, Foundation of Research and Technology Hellas (FORTH), 26504 Patras, Greece
* Correspondence: abougiat@noa.gr

**Abstract:** This study provides an overview of the atmospheric drivers of climate change over Greece (Eastern Mediterranean), focusing on greenhouse gases (GHG: carbon dioxide, $CO_2$; methane, $CH_4$; etc.). $CO_2$ in Greece is mostly produced by energy production, followed by transport, construction, and industry. Waste management is the largest anthropogenic source of methane, accounting for 47% of total $CH_4$ emissions, surpassing emissions from the agricultural sector in 2017, while the energy sector accounts for the remaining 10.5%. In situ simultaneous observations of GHG concentrations in Greece conducted at three sites with different topologies (urban background; Athens, regional background; Finokalia and free troposphere; and Helmos) during the last 5 years (2019–2023) showed increasing trends of the order of 2.2 ppm·yr$^{-1}$ and ~15 ppb·yr$^{-1}$ for $CO_2$ and $CH_4$, respectively, in line with the global trends. These increasing trends were found from both ground-based and satellite-based remote-sensing observations. Finally, during the lockdown period due to the COVID-19 global pandemic, a 58% reduction in $CO_2$ levels was observed in the urban background site of Athens after subtracting the regional background levels from Finokalia, while the respective reduction in $CH_4$ was of only the order of 15%, highlighting differences in emission sources.

**Keywords:** carbon dioxide; methane; trends; East Mediterranean; COVID-19



**Citation:** Bougiatioti, A.; Gialesakis, N.; Sarafidis, Y.; Gini, M.I.; Mermigkas, M.; Kalkavouras, P.; Mirasgedis, S.; Ramonet, M.; Narbaud, C.; Lopez, M.; et al. Sources and Variability of Greenhouse Gases over Greece. *Atmosphere* **2024**, *15*, 1288. https://doi.org/10.3390/atmos15111288

Academic Editor: László Haszpra

Received: 2 September 2024
Revised: 23 October 2024
Accepted: 24 October 2024
Published: 27 October 2024



## 1. Introduction

Greenhouse gas (GHG) is any gas that has the property of absorbing infrared radiation emitted from Earth's surface and reradiating it in different directions, so that some of it is trapped in the Earth's atmosphere and is contributing to the greenhouse effect. Carbon dioxide, methane, and water vapor are the most important greenhouse gases. The rapid human-driven increase in greenhouse gas (GHG) is the main factor responsible for the rise in global temperature observed since the industrial revolution. Together, $CO_2$ and $CH_4$ contribute approximately 87% to the global warming induced mainly by human-driven emissions of GHG ($CO_2$, $CH_4$, $N_2O$, and CFCs) since the preindustrial era [1]. Atmospheric $CO_2$ concentrations have been recorded at the Mauna Loa Observatory in Hawaii since 1958. This is the longest modern atmospheric record. Between 2000 and 2020 the growth rate has

been on average 2.20 ± 0.46 ppm per year, and the last three years average (2021–2023) 2.52 ± 0.65 ppm per year [2]. In addition, 2023 was the 12th year in a row with an annual rise of $CO_2$ by more than 2 ppm [3]. Since the middle of the 20th century, annual emissions from burning fossil fuels have grown every decade, from close to 9.4 billion tons of carbon dioxide per year in 1960 to 37.2 billion tons in 2022, while land-use emissions decreased from 7.9 ± 3.5 to 6.1 ± 2.2 billion tons, respectively, according to the Global Carbon Budget 2023 [4].

According to the Global Carbon Project 2023 [4], global fossil $CO_2$ emissions have augmented by an average of 2.8% $yr^{-1}$ between 2000 and 2009, and then, after a decline due to the global financial crisis, they increased by 1% $yr^{-1}$ until 2019 before declining by 5.7% during the COVID-19 pandemic and increasing to 37.1 ± 2 billion tons of $CO_2$ per year ($GtCO_2 \cdot yr^{-1}$) in 2022. Coal, oil, gas, cement, gas flaring and others contribute 41%, 32%, 21%, 4%, and 2%, respectively, to the global fossil emissions. It is worth noting that Europe's per capita $CO_2$ fossil emissions have been decreasing since 1980 and were 6.2 tons per person in 2022, less than half that of the United States, while those of China and India are rising. Land use change is the other major source of $CO_2$ partially controlled by humans, which has been decreasing over the last two decades and is estimated to average 4.7 ± 2.6 billion tons of $CO_2$ $yr^{-1}$ over the period 2013–2022. Carbon dioxide's lifetime in the atmosphere is controlled by its uptake by terrestrial vegetation and the ocean and is of the order of a few hundreds of years.

For the past decade, atmospheric inversion estimated global $CH_4$ emissions to be 575 Tg $CH_4$ $yr^{-1}$ (ranging between 553 and 586) with ~65% (63–68%) of these emissions due to direct anthropogenic sources (fossil fuel use, agriculture and waste management, and anthropogenic biomass burning), wetlands, and other natural emissions, including termites and permafrost [5]. Based on a globally distributed network of sampling sites, the NOAA's Earth System Research Laboratory monitors the annual growth of $CH_4$ levels since 1983, which on 2021 hit a record of 17.92 ± 0.45 ppb [6]. Methane reacts with hydroxyl (OH) and chlorine (Cl) radicals in the atmosphere and is also removed from the atmosphere by methanotrophic bacteria in soils. Methane's average lifetime is 9.8 ± 1.6 years [7], which is at least an order of magnitude shorter than that of $CO_2$. In addition, methane is more effective than $CO_2$ at absorbing thermal infrared radiation per unit mass. Thus, $CH_4$ has a global warming potential (GWP) 86 times higher than $CO_2$ in a 20-year timescale and 28 times stronger on a 100-year timescale [8]. Due to the relatively short lifetime and large GWP of methane, $CH_4$ is a good candidate GHG for short-term climate change mitigation. This is very important, since based on the Global Methane Pledge [9], a global initiative in which currently 155 countries are participating, and amongst these is Greece, the aim is to reduce methane emissions by 30% by the year 2030. Furthermore, on November 2023, a provisional agreement was reached between the European Parliament and Council on a new EU Regulation to reduce energy sector methane emissions in Europe and in the global supply chains. This agreement is, therefore, crucial to delivering the European Green Deal and reducing net greenhouse gas emissions by at least 55% by 2030. The agreement requires formal adoption by both the European Parliament and the Council. Once this process is completed, the new legislation will be published in the Official Journal of the Union and enter into force [9].

Regionally, in climate-sensitive areas, like the Arctic and the Mediterranean, temperature changes can be faster than the global mean [10]. The Eastern Mediterranean is a region with high aerosol loads from both natural and anthropogenic sources and diminishing water resources that are exacerbated by high aerosol loads and climatic change [11,12]. A recent study [13] highlights that the Eastern Mediterranean and Middle East region has warmed around twice faster than the global average temperature increase (0.45 °C/decade versus 0.27 °C/decade globally) for the period between 1981 and 2019. This faster warming is found to be characteristic of the last 2 decades, and it is partly attributed to a significant reduction in aerosols, especially sulfate, which has a cooling effect, motivated by clean air policy [14]. Since temperature variability is highly dependent on regional factors such as

changes in incoming radiation, radiative forcing by natural and anthropogenic GHGs, and more localized features such as aerosol pollution and the presence of mineral dust, the decreasing trend in cooling aerosols and increasing GHG in the region, together with the drop in soil moisture in the eastern Mediterranean basin, are found to be the main drivers of the rapid temperature rise over the last two decades in the region [14]. The rise of the average temperature that is experienced in the region is accompanied by more frequent extreme weather events such as heat waves, prolonged droughts, and heavy rainfall, which are indicative of climate change [13].

Greece in the Eastern Mediterranean is committed to reduce GHG emissions and comply with EU recommendations. In recent years, a strong monitoring network has been established to systematically map GHG levels in Greece (Figure 1). The present study provides, for the first time to our knowledge, an overview of Greek emissions as well as GHG observations from in situ, complemented by ground-based remote sensing and satellite measurements, covering a wide range of locations from regional background sites to urban sites. Trends are identified and verified by the different observational means combined in this study, and possible causes are proposed for these observed trends.

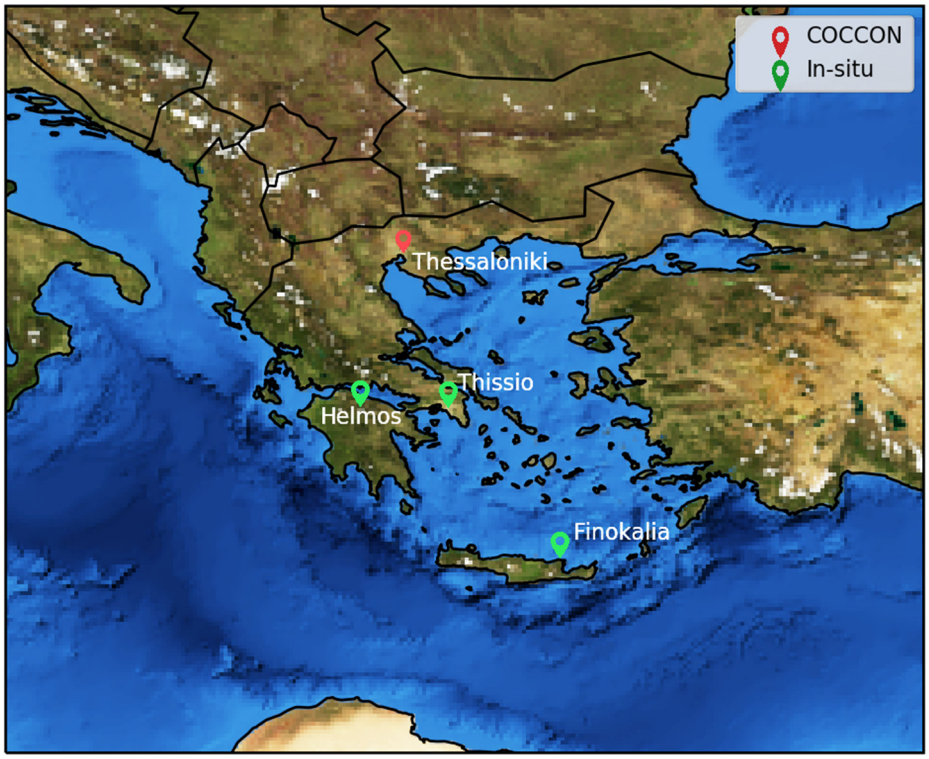


**Figure 1.** Sites for GHG observations in Greece. Observatories with in situ measurements of GHG (green) and COCCON remote sensing observations (red).

## 2. Materials and Methods

### *2.1. Emission Database Methodology*

GHG emission inventories are derived from the official submissions of Greece to the United Nations Framework Convention on Climate Change (UNFCCC), according to all relevant UNFCCC decisions. Methods used to calculate emissions are based on the 2006 IPCC Guidelines for National Greenhouse Gas Inventories [15] (as updated), while activity data and emission factors used are described and presented in the documents submitted to the UNFCCC.

### *2.2. Observations*

For the real-time continuous in situ near-surface measurements of $CO_2$ and $CH_4$ in this study (Finokalia, Helmos, and Thissio/Athens; Figure 1), cavity ring-down spectrom-

eter (CRDS) Picarro G2401 analyzers with a 1 sec time resolution [16] were used [10,17], following the Integrated Carbon Observation System (ICOS) specifications [18,19]. The analyzers were calibrated according to the WMO-X2007 and WMO-X2004A reference scales for $CO_2$ and $CH_4$, respectively. In addition, one target cylinder of known $CO_2$ and $CH_4$ concentrations has been measured twice a day for quality assurance/quality check purposes in Athens and Finokalia, respectively. During the measurement period in Athens (2019–2023), four target cylinders were operated in the measurement site, with the last one over a period of almost 20 months (August 2022 to May 2024) averaging at 418.88 ± 0.015 ppm for $CO_2$ and 1945.307 ± 0.075 ppb for $CH_4$, compared to assigned averages of 418.97 ± 0.008 and 1945.31 ± 0.042, respectively. For the Finokalia data, a similar setup was used, and a short-term variability of 0.1 ppm for $CO_2$ and 1 ppb for $CH_4$ is observed with the target cylinders used [10].

Long-term GHG monitoring in Greece commenced at the Finokalia Observatory (35°20′ N, 25°40′ E, 250 m a.s.l.). Finokalia is the atmospheric research station operated by the University of Crete and is located 50 km east of Heraklion, the largest city of the island. Observations from this station have been used extensively to characterize the regional background atmospheric composition of the Eastern Mediterranean [20,21]. Since 2002, glass flasks were collected on a weekly basis and were subsequently sent for analysis in France (LSCE, Gif-sur-Yvette, France) using a commercial gas chromatograph (6890 N, Agilent Technologies; Santa Clara, CA 95051, USA) equipped with a flame ionization detector, adapted for flask analyses. Real-time continuous measurements of $CO_2$, $CH_4$, and $H_2O$ at Finokalia were started in 2014 using a Picarro G2401 (Picarro Inc., Santa Clara, CA 95054, USA) [16]. Continuous GHG measurements in the urban environment of Athens were started in January 2019 at the premises of the National Observatory of Athens (NOA) (37.97° N, 23.72° E, 110 m a.s.l.) located in downtown Athens, using also a Picarro G2401 as at Finokalia and the same calibration protocol. At the Helmos Hellenic Atmospheric Aerosol and Climate Change station (HAC)[2] (37.98° N, 22.19° E, 2314 m a.s.l.) operated by NCSR Demokritos, GHG measurements are also performed using a Picarro G2401 since 2016.

Furthermore, the total column of trace gases at Thessaloniki is measured by Fourier-transform infrared (FTIR) spectrometers using the direct solar radiation as a light source. The COllaborative Carbon Column Observing Network (COCCON), established in 2014, aims to increase global coverage of GHG columnar observations [22]. COCCON uses the Bruker EM27/SUN portable low-resolution FTIR spectrometer [23], developed by KIT in collaboration with Bruker Optics™ (Billerica, MA 01821, USA), as a mobile, reliable, easy-to-deploy, and low-cost supplement to the Total Carbon Column Observing Network (TCCON) high-resolution spectrometers [24]. The EM27/SUN is stable on timescales of several years; the drift per year between the EM27/SUN and the official TCCON product is 0.02 ppmv for $XCO_2$ and 0.9 ppbv for $XCH_4$, which is within the 1σ precision of the comparison, 0.6 ppmv for $XCO_2$, and 4.3 ppbv for $XCH_4$ [22]. The EM27/SUN is a portable, ground-based, direct solar-viewing low-resolution (0.5 $cm^{-1}$) Fourier-transform spectrometer intended to measure direct solar radiation in the near infrared (NIR) spectral range. The spectral resolution of this instrument is similar to that of TROPOMI, S-5P's spaceborne sensor. During clear sky days, with a scanner velocity of 10 kHz and 10 scans, each spectrum and subsequently total column measurements of GHGs are obtained within approximately 58 s. Thus, the co-located pixels can differ from measurement to measurement. For the Thessaloniki FTIR ground-based instrument, which is co-located with the S5P measurements, an average of many S5P pixels can improve the statistical significance of the data because ground-based sites located close to a sea/ocean coast will always lack S5P $CH_4$ pixels over water.

Finally, level 2 columnar retrievals of $CH_4$ provided by the Sentinel-5 Precursor TROPOspheric Monitoring Instrument (TROPOMI), available since April 2018, are also used for the present analysis.

### *2.3. Trend Analysis*

All trends were calculated from deseasonalized data, and all the trends have been identified as statistically significant from the Mann–Kendall test. The method for the removal of seasonality is described in Gialesakis et al. [10]. The growth rate is calculated for each species using the method described by NOAA [25]. For $CO_2$, deseasonalized data for each station were used. For each year, a 4-month average (November–February) was used, and the growth rate was calculated by subtracting the average of the wanted year from the average of the following year.

$$2019\ Growth\ Rate = 2020_{(November-February)} - 2019_{(November-February)} \quad (1)$$

For $CH_4$, the mean monthly time series were deconstructed to trend, seasonality, and residuals [10]. The growth rate is calculated by subtracting the January value of the wanted year from the January value of the following year.

## 3. Results and Discussion

### *3.1. Greenhouse Gas Emissions*

#### 3.1.1. GHG Emissions in Greece

Total GHG emissions in Greece, excluding emissions and removals from Land Use, Land Use Change, and Forestry (LULUCF), as well as emissions from international maritime shipping and aviation, are reported in Figure 2. The uncertainty for GHG emissions per gas in 2021 was estimated to be 2.5% for $CO_2$ emissions, 23.8% for $CH_4$ emissions, 109.7% for nitrous oxide ($N_2O$) emissions, and 260.1% for the F-gas emissions [26]. The total uncertainty is about 12.5% (excluding LULUCF), while the uncertainty carried over into the GHG emissions trend is 9.1%.

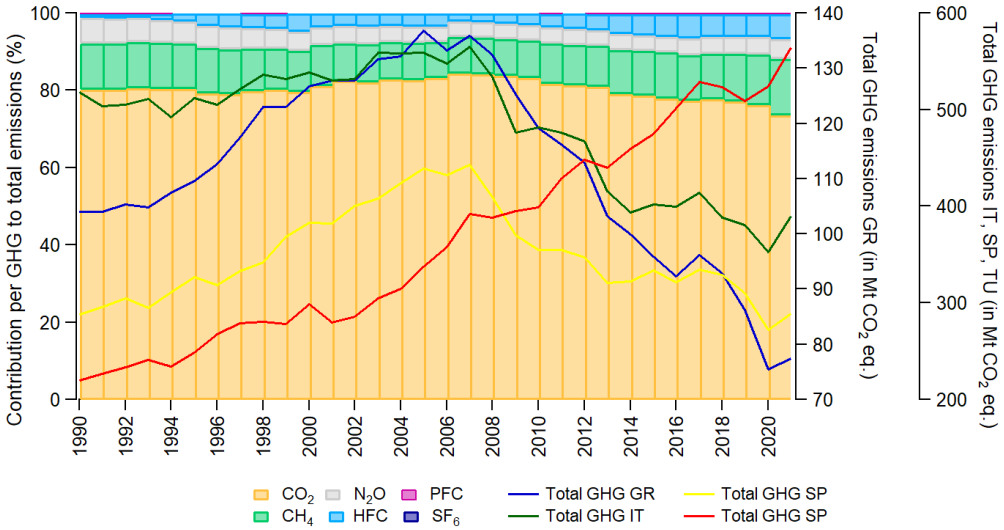


**Figure 2.** Total GHG emissions in Greece (in Mt $CO_2$ eq.) for the period 1990–2021 (excluding LULUCF) (right *y*-axis, blue line) and for Italy, Spain, and Türkiye (secondary right *y*-axis, green line, yellow line, and red line, respectively) and contribution per greenhouse gas in Greece (left *y*-axis and bars) [26].

They weakened by about 25% from 103.99 Mt $CO_2$ eq. in 1990 to 77.49 Mt $CO_2$ eq. in 2021 (Figure 2). Compared to 1990, EU net GHG emissions in 2021 were 30% lower, while preliminary estimates indicate that net GHG emissions in 2022 were a further 1.9% lower than in 2021, largely due to the energy crisis [27]. Considering the contribution of the LULUCF sector, net emissions drop by about 29% from 101.74 Mt $CO_2$ eq. in 1990 to 72.01 Mt $CO_2$ eq in 2021.

Emission trends follow three different patterns [26]. From 1990 to 1993, GHG emissions remained fairly constant with an average annual growth rate of 0.27%, which accelerated to

1.57% per year between 1993 and 2008. Then, a sharp decline (−4.04%) took place between 2008 and 2021 due to not only economic recession and climate change policies and measures but also the impact of the COVID pandemic (especially for 2020 emissions). According to a recent study [28], a reduction in emissions should be expected in 2020 as a result of a decline in electricity consumption, road and navigation transport sector activity, and a surge in the use of diesel oil and natural gas, mostly for heating and for other uses in the residential and tertiary sectors. The lockdown effect on GHG and air pollutants in Greece is analyzed in Section 3.4.

Emissions from international transport are not accounted for in the context of reduction targets established under the United Nations Framework Convention on Climate Change (UNFCCC) but are monitored and reported separately (as memo items) in the official inventory submissions. In 2021, emissions from international transport are estimated to be 8.63 Mt $CO_2$ eq., 20% lower than in 1990. Between 1990 and 2005, the emissions from international aviation almost doubled, and from 2005 to 2019, they further augmented by 39% [27].

In Figure 2, there is a clear reducing trend in the amount of GHG emissions after 2007. Similarly, a clear reduction trend can be seen in the total amount of GHG emissions for other southern European countries, such as Italy and Spain, based on the UNFCCC inventory submissions. When comparing the periods 1990–2007 and 2008–2021, the mean values for the two periods exhibit a 15% reduction for Greece, a 19% decrease for Italy, a 7.5% for Spain, and a 66% rise for Türkiye [29]. The reduction in the European countries can be associated with the 2007 goal leaders set for a 20% reduction in EU GHG emissions by 2020 compared to emissions in 1990. Based on the data, Greece achieved a 27% reduction in 2020 compared to emissions in 1990, Italy achieved a 32% reduction, Spain achieved a mere 5% reduction, and Türkiye had a strong growth of 139%.

#### 3.1.2. Emissions per Greenhouse Gas

Carbon dioxide ($CO_2$) emissions represent the majority of GHG emissions in Greece (Figure 2). On average, the contribution of $CO_2$ emissions to total GHG emissions is estimated at 80%. In 2021, $CO_2$ emissions account for 74.3% of total emissions (excluding LULUCF) and are 31% lower than in 1990. Fossil fuel consumption in the energy industry (power generation and refineries) and in the final energy demand sectors are the main sources of $CO_2$ emissions, accounting for more than 90% on average over the period from 1990 to 2021. More specifically by sector, it can be seen in Figure 3a that electricity and heat contribute 50% of the GHG emissions in tons of $CO_2$ eq., followed by transport (22%), and manufacturing and construction (9.5%). Lower quantities of $CO_2$ are generated from buildings and waste incineration sectors.

The share of $CH_4$ emissions to total GHG emissions is 14.6% in 2021 (Figure 2). Methane emissions subsided by 10% between 1990 and 2021, while accounting for 11% of total GHG emissions on average (in $CO_2$ equivalent). Agriculture (mainly enteric fermentation, but also manure management) and waste (solid waste disposal on land in managed or unmanaged sites) are the main sources of emissions, with a contribution (in 2020) of about 42% and 48%, respectively (Figure 3b). More specifically, waste as a source of $CH_4$ has surpassed the emissions from agriculture since 2017, with 4.3 Mt of $CO_2$ eq. compared to 3.91 Mt of $CO_2$ eq. Lignite mining is the main source of methane emissions from the energy sector (3% in 2020). This contribution is expected to be zero by the end of this decade due to the phaseout of lignite-fired power plants.

Nitrous oxide ($N_2O$) is another greenhouse gas, for which the contribution to total GHG emissions is estimated at 5% [26]. Agriculture is the main source of $N_2O$ emissions, as agricultural activities add nitrogen to soils (i.e., in the form of synthetic nitrogen fertilizers). Fossil fuel combustion contributes also to $N_2O$ emissions, while the contribution of the waste sector (mainly wastewater handling) has almost doubled since 1990. Since $N_2O$ measurements are scarce in Greece (e.g., [30]), the main focus of the current study is $CO_2$ and $CH_4$, which are also the main contributors to GHG emissions.

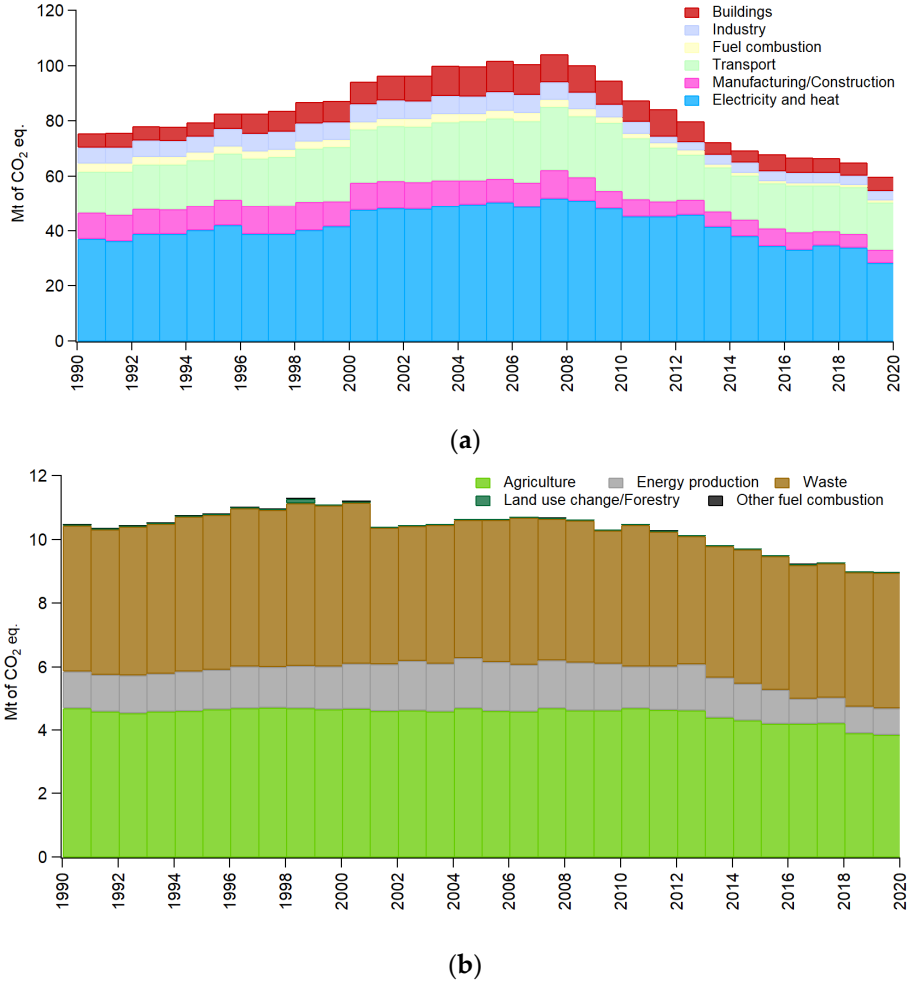


**Figure 3.** Interannual variation of sectoral emissions of $CO_2$ (**a**) and $CH_4$ (**b**) in Greece (in Mt of $CO_2$ eq.) over the period from 1990 to 2020.

### 3.1.3. Greenhouse Gas Emissions per Sector

At the sectoral level, activities included in the energy sector account for the majority of GHG emissions in Greece over the period from 1990 to 2021 (Figure 4), which follows the emissions profile of the developed countries (i.e., countries included in Annex. I of the UNFCCC). In Greece, the contribution of the energy sector ranges from 68.5% (2020) to 80.2% (2009). On absolute terms, emissions from the energy sector peaked in 2007 (108.3 Mt $CO_2$ eq.) and are 30.5% lower in 2021 than in 1990. Within the energy sector, electricity generation and road transport account for about 70% of the sectoral emissions in the period from 1990 to 2021. Electricity generation is the main source of GHG emissions in Greece, accounting for about 40% of total GHG emissions in 1990 and for 26% in 2021. In contrast, emissions from road transport grew by 21% from 1990 to 2021.

In contrast, emissions from the agriculture sector are 23.6% lower in 2021 than in 1990 (8.05 Mt $CO_2$ eq. against 10.53 Mt $CO_2$ eq., respectively), while its contribution presents a marginal change from 10.1% in 1990 to 10.4% in 2021. The reduced use of synthetic nitrogen fertilizers and the reduction in livestock population are among the main parameters that have shaped emissions from agriculture in Greece. According to the National Inventory Report [26], the synthetic nitrogen applied to soils shrank from 424 kt in 1990 to 182.65 kt in 2021.

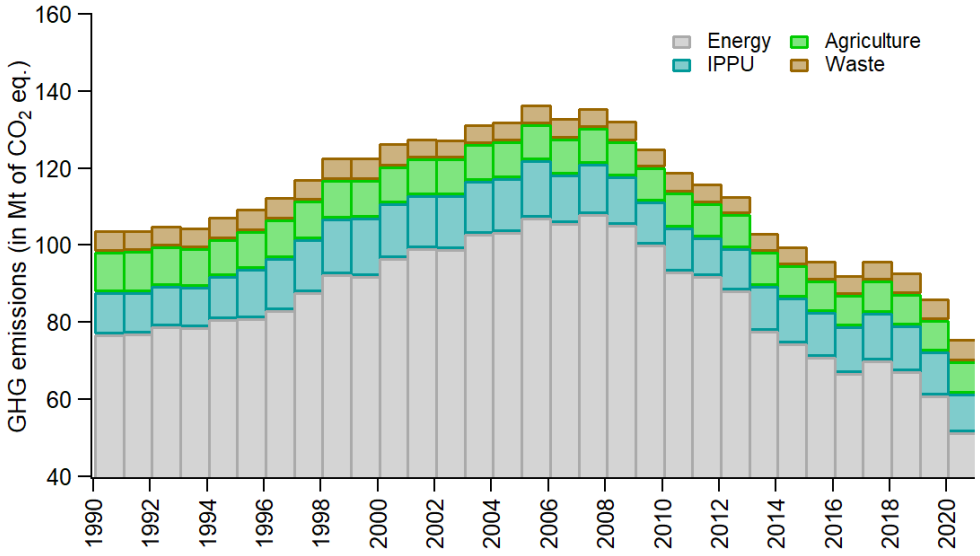


**Figure 4.** Total GHG emissions per sector in Greece (in Mt $CO_2$ eq.) for the period 1990–2021, excluding LULUCF [26].

Emissions from the waste sector (5.85 Mt $CO_2$ eq.) are 8.7% higher in 2021 than the 1990 levels. Since 1994, solid waste disposal on land is the main source of emissions within the sector, and relevant emissions increased by 67% from 1990 to 2021. Considering that landfilling is still the main treatment operation for municipal solid waste (91% of the quantities generated were landfilled in 1990 and 82% in 2021) and that the waste generation rate has been increasing [26], this is an expected development. The contribution of wastewater handling activities to total emissions is decreasing (from 53.9% in 1990 to 29.4% in 2019), as the share of population served from aerobic wastewater handling is increasing and reached 91% in 2019 [26].

LULUCF was a net sink of GHG during the period from 1990 to 2021. Net removals ranged from 0.61 kt $CO_2$ eq. (2014) to 5.48 Mt $CO_2$ eq. (2021). These variations are the result of the rise in the sink capacity of the Forest Land and Cropland category [26].

### *3.2. An Assessment of Emission Trends in the Energy Sector*

Fuel combustion activities are the main source of GHG emissions in Greece and in the developed countries, in general. On average, emissions from the energy sector account for about 80% of total GHG emissions over the period from 1990 to 2021, excluding LULUCF. It is, therefore, important to highlight and explain the multi-year changes in this sector, as they have a significant impact on the overall GHG emission trends.

The decomposition analysis has been widely used to identify and quantify the drivers of change in GHG emissions, including in the IPCC Assessment Reports [31]. The main methods used are the Structural Decomposition Analysis (SDA) and the Index Decomposition Analysis (IDA), where SDA uses the input–output model and the IDA method exploits commonly used aggregated data to decompose indicator changes [32].

In the context of the present analysis, the IDA method was applied in the form of the Kaya identity that decomposes changes in GHG emissions from the energy sector into four driving factors, namely, population, gross domestic product (GDP) per capita, energy intensity (primary energy consumption per GDP), and the carbon intensity of the energy mix (GHG emissions per primary energy consumption) (Equation (2)) as follows:

$$\text{Emissions} = \text{Population} \times \frac{\text{GDP}}{\text{Population}} \times \frac{\text{Primary energy}}{\text{GDP}} \times \frac{\text{Emissions}}{\text{Primary energy}} \quad (2)$$

Data used are derived from official statistics as presented in EUROSTAT (population and primary energy consumption) and the AMECO database (gross domestic product) [33],

and calculations are made on the basis of the Laspeyres method that isolates the impact of a variable by letting that variable change and keeping the other variables constant.

Based on the results from the analysis (Figure 5), the reduction in GHG emissions from the energy sector (31%) can be decomposed into changes in population (+6%), GDP per capita (+20%), energy intensity (−25%), and carbon intensity of energy (−26%) between 1990 and 2021. Applying the Kaya identity separately for the emission increasing period (1990–2008) and the emission decreasing period (2008–2021) highlights differences on the relevant contribution but also on the sign (positive or negative contribution) of the examined factors to explain emissions trends in the energy sector (Figure 3). The main findings are as follows:

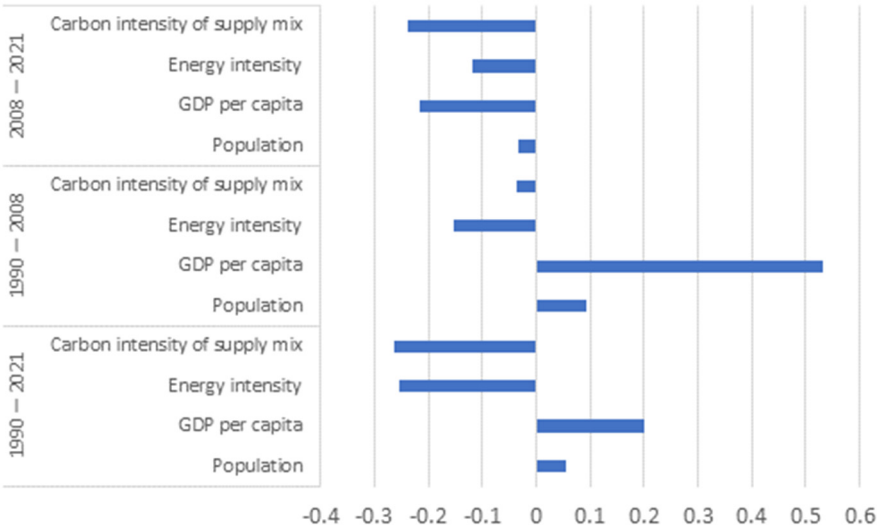


**Figure 5.** Applying the Kaya identity for 1990–2019 (total period), 1990–2008 (rise in emissions), and 2008–2021 (decrease in emissions).

- During the period of emissions increase (1990–2008), population had a positive effect on emissions (+9%), while during the period of emissions decrease (2008–2019), this influence became negative (−3%), as the population of Greece plunged after 2011. In total, the population retains the positive effect (+6%) for the whole period (in which emissions dropped).
- Economic development, as depicted in the GDP per capita indicator, was the single most important factor explaining the rise in emissions during the 1990–2008 period, with a value of +53%. The influence became negative in the subsequent period (economic recession), with a value of −22%. In total, the effect of economic development is positive (+20%).
- The contribution of energy intensity was negative for all the periods considered, that is, energy intensity contributes to a lower growth of emissions. The effect was greater during the 1990–2008 period with a value of −15%, as compared with a value of −12% in the 2008–2021 period. The effect of energy intensity is related to improvements in energy efficiency due to the penetration of natural gas, the extended use of renewable sources in the Greek energy system, and the reduced activity of energy-intensive industries during the period of the economic recession.
- The contribution of the carbon intensity of the energy supply mix is also negative for all the periods considered. The contribution was minor during the first period (−3%) and became more significant during the second period (−24%). During the whole period (1990–2021), the effect of carbon intensity is negative with a value of −26%. Up to 2008, the most notable change in the Greek energy system was the introduction of natural gas not only in electricity generation but also in final energy demand sectors and especially industry. During the whole period (1990–2019), the effect of carbon intensity is negative with a value of −23%. Since 2008, the share of renewable sources

in electricity generation grew from 9.65% to 31.3% in 2019 and 35.93% in 2021, as estimated by the SHARES tool that focuses on the harmonized calculation of the share of energy from renewable sources [34].

Summarizing, during the period of economic growth, the increase in emissions was mainly the result of economic development, while during the economic recession period, the reduction in emissions was the result not only of the reduction in economic growth but also of the improvement in the carbon intensity of the supply mix. It is the latter that should be retained and enhanced towards a low/zero carbon economy, together with improvements on the energy intensity of the Greek economy.

### *3.3. Recent Observations and Trends of Greenhouse Gases in Greece*

#### 3.3.1. In Situ Greenhouse Gas Observations

The regional and global variability of the parameters affecting climate change and the variability and extent of transboundary air pollution in Europe require the study of aerosol properties and the variability of GHG at background conditions, which can be ensured at remote surface or high-altitude sites. High-altitude observatories are mostly in the free troposphere with very little influence from the atmospheric boundary layer [35]. Finokalia monitoring station in Lasithi, Crete, is a coastal remote location representative of boundary layer regional background conditions in the eastern Mediterranean [20,21]. The Helmos HAC Observatory is one of the very few high-altitude atmospheric monitoring stations in Europe and the only one at high altitude for atmospheric research in the region of the eastern Mediterranean [36]. Thissio Observatory in the center of Athens provides information on urban background GHG levels, and by comparison to the regional background, the contribution of the city to GHG levels can be derived [17].

**Trends.** The longest data series of $CO_2$ and $CH_4$ observations in the eastern Mediterranean has been recorded at the Finokalia Observatory. Based on the more than twenty-year record of measurements at Finokalia (Figure 6a), $CO_2$ concentrations augmented by 2.4 ppm·yr$^{-1}$ between 2002 and 2023, following the average rate of growth of $CO_2$ in the north hemisphere as calculated from NOAA observations, similar to that observed at Mauna Loa in the middle of the North Pacific. Over the same period, $CH_4$ climbed by an average of 8.6 ppb·yr$^{-1}$ at Finokalia (Figure 6b), but the increase has accelerated since 2018 (13.1 ppb·yr$^{-1}$) [10]. $CH_4$ levels at Finokalia are higher than those observed at Mauna Loa (Figure 6b) as well as the north hemisphere mean, most probably reflecting regional emissions of $CH_4$ in the eastern Mediterranean [10]. Overall, a steadily increasing trend of $CO_2$ and $CH_4$ levels was observed in Greece during the last years (Figure 7). Indeed, an average rise of 2.4 ppm·yr$^{-1}$ ($CO_2$) and 11.8 ppb·yr$^{-1}$ ($CH_4$) was observed from 2016 to 2021 at HAC Observatory (Figure 7a,b). Especially in the HAC Observatory, $CH_4$ grew by 3.2 ppb·yr$^{-1}$ from 2016 to 2018 and by 13.2 ppb·yr$^{-1}$ since 2018 (Figure 7b). In Athens, $CO_2$ concentrations increase by 2.3 ppm·yr$^{-1}$ (2019–2023), similar to the surge at the other two locations for the same time period. $CH_4$ showed a mean increasing trend of 14.2 ppb·yr$^{-1}$ between 2019 and 2023, comparable to the increase observed at Finokalia (13.7 ppb·yr$^{-1}$) and Mount Helmos (14.0 ppb·yr$^{-1}$) for the same period (2019–2023).

Based on a recent study focusing on livestock economy in Greece [37] on the data retrieved from the official site of the Greek Payment and Control Agency for Guidance and Guarantee Community Aid (OPEKEPE), it occurs that there has been a sharp increase in animal population since 2018–2019, which could eventually be reflected in GHG emissions. More specifically, between the years 2011 and 2021, the regions of Western Macedonia, Epirus, Thessaly, Western Greece, and Central Greece have recorded a rise of 81, 69.5, 67, 59.6, and 39.6%, respectively, in total GHG emissions, which could partially explain the local trend in $CH_4$ levels, especially since 2018.

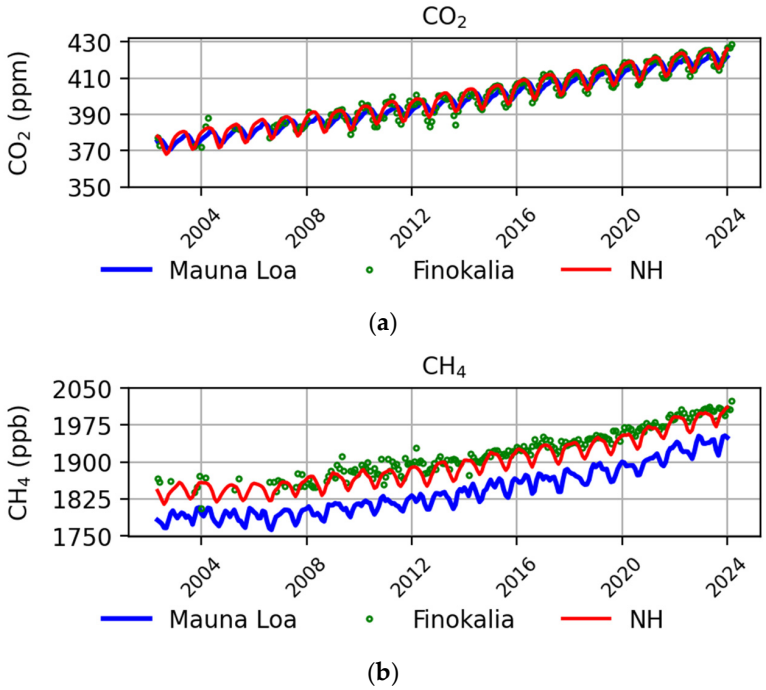


**Figure 6.** Interannual variability of atmospheric $CO_2$ (**a**) and $CH_4$ (**b**) levels at Finokalia (green symbols) and comparison with observations from Mauna Loa (blue line) and the north hemisphere mean from NOAA flask measurements (red line) during the same period.

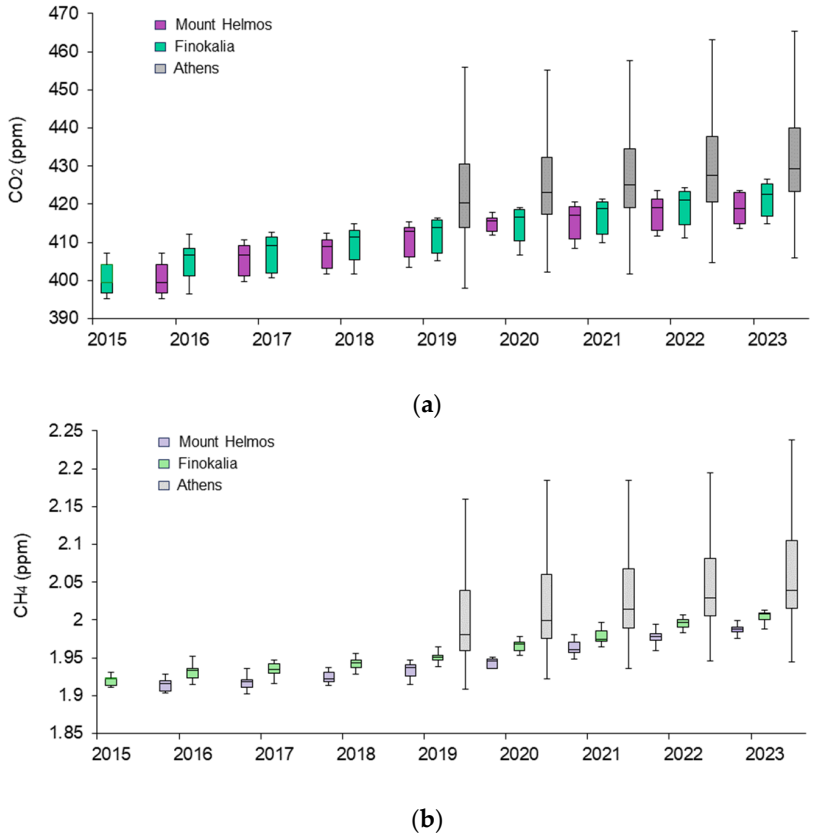


**Figure 7.** Frequency distribution of atmospheric $CO_2$ (**a**) and $CH_4$ (**b**) concentrations at the three monitoring stations: Finokalia (green), Mount Helmos (violet), and Athens-Thissio (gray).

Based on the annual increase in the globally averaged atmospheric $CH_4$ levels as recorded by the NOAA's globally distributed network of air sampling sites [38], the year

2021 exhibited a record rise of 17.91 ppb [6]. Nevertheless, globally, there was also a significant growth in 2020 (from 1 January 2020 to 31 December 2020, 15.15 ppb). In Greece, in 2020, $CH_4$ at Finokalia exhibited a 12.6 ppb increase lower than that observed in Athens (19.6 ppb) and comparable to the one observed at Mount Helmos (15.7 ppb). The surge was also high and almost the same in 2021 in Finokalia and Mount Helmos (~19 ppb) and half in Athens (8.1 ppb). However, in 2022, in Finokalia, the climb was quite lower (11.2 ppb), while it was 15.8 ppb in Thissio and 9.4 ppb in Mount Helmos.

**Seasonal variability.** On a global scale, the seasonal variability of $CO_2$ reflects the breathing of the biosphere, with the highest concentrations in spring and the lowest ones in summer [39]. The seasonal amplitude of $CO_2$ is thus expected to be the largest in areas with significant vegetation. This is clearly seen in Figure 6, where the seasonality of $CO_2$ at Finokalia Observatory in the middle of the Eastern Mediterranean is similar to the seasonality of the North Hemisphere average from the NOAA stations and with greater amplitude than that observed at the Mauna Loa Observatory in the middle of the North Pacific. At the background sites (coastal, Finokalia, and high altitude, Helmos), it is clear that there is similar seasonal variability in both $CO_2$ and $CH_4$, with levels at Helmos generally somewhat lower due to the fact that it is a free troposphere station. At these sites, $CO_2$ shows maxima in early spring and minima in summer (Figure 8a). $CO_2$ levels in the urban background environment of Athens also reach a minimum during the summer, exhibiting values similar to those at the background sites. This is in agreement with aerosol observations indicating that during the summer, Greece and generally the Eastern Mediterranean are affected mainly by regional rather than local sources [40]. Moreover, $CO_2$ in Athens shows a pronounced maximum during winter, exhibiting more than 20 ppm higher values than during summer, mostly attributed to the additional anthropogenic source for heating purposes of the Greek capital [41] (Figure 8a).

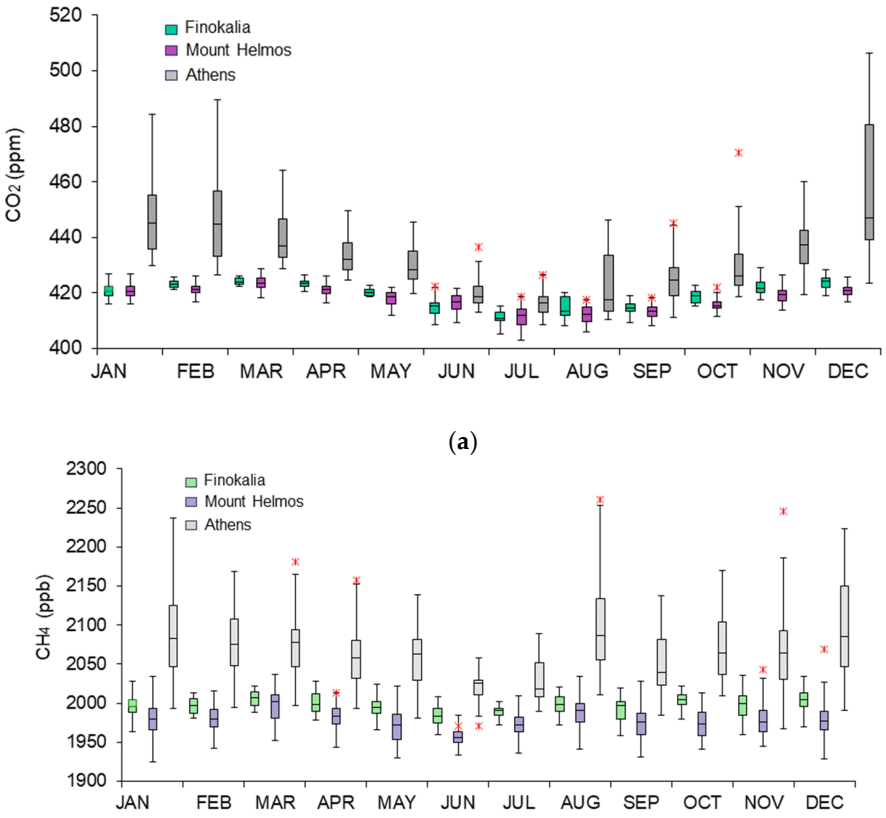


**Figure 8.** Seasonal variability of atmospheric $CO_2$ (**a**) and $CH_4$ (**b**) concentrations in Athens (gray), Finokalia (green), and Mount Helmos (violet) for the year 2022. Red asterisk represent outliers.

This is not the case for $CH_4$ in Athens, which shows elevated values all over the year (Figure 8b), with no clear seasonal variability, as it was also observed for $CH_4$ at Finokalia. Moreover, $CH_4$ in Mauna Loa shows a clear seasonal cycle (Figure 6b), which is due to the location of the observatory and the lack of local/point sources and is representative of a globally averaged background mean.

The seasonal variability of $CH_4$ (Figure 8b) shows a small maximum in winter/spring, which could be due to emission sources, as agriculture can be a significant contributor. Minimum concentrations are observed in summer, when photochemistry in the region is intense [10]. In Athens, however, apart from higher concentrations, the sources may also be different, as emissions from the waste sector have surpassed those from agriculture since 2017 (Figure 3b and Section 3.1.2). Athens is the capital of Greece, with almost half the Greek population living in the metropolitan area; therefore, waste and energy production are the sectors that drive $CH_4$ levels in Athens. These are the highest in the summer (August) and December, when these two sources are expected to contribute the most due to tourism and therefore increased waste in the summer and heating in the winter.

**Urban sources of GHGs.** Recently, GHGs measurements in the urban environment of Athens, Greece, have revealed that both gases exhibit maxima in winter, with enhanced levels during night and early morning hours being attributed to traffic/heating emissions and leakages of residential natural gas for $CO_2$ and $CH_4$, respectively [17], amplified also by the low boundary layer height, favoring the accumulation of pollutants near the surface. Although $CO_2$ showed an excellent correlation with CO and black carbon (BC), indicating its main origin from combustion sources, this was not the case for $CH_4$, which showed at least two different subsets of data, one of which showed a good correlation with CO, indicating a common source (combustion). Other possible sources may include leakages from natural gas transmission pipelines and landfills. Landfills in particular have been shown to be a significant contributor to local methane emissions. In order to evaluate the additional load from anthropogenic sources in the urban environment of Athens, where the biospheric respiration is minimal, the levels of the two GHGs were directly compared with the respective observations at the Finokalia Observatory, considered background values. Thus, the difference between the two sets of values is considered the increment associated with the anthropogenic input. It was found that for a 5-year period (2019–2023), the additional load due to the anthropogenic activities plus the effect of the biospheric fluxes in the urban environment is on average of the order of 2.7%. When considering the monthly variability, the $CO_2$ difference between the mean values for the two sites ranges between 3% and 7.5% (or between 14 and 32 ppm) during winter (which during nighttime may even reach 20%, which translates to more than 110 ppm), while during summer, the differences are minimal (ranging between 0.5% and 2.2%). For $CH_4$, the additional burden due to the urban environment and activities is once again of the order of 3.3% (or 68.3 ppb) for the whole 5-year period (ranging between 1.2 and 5.4%) but without a notable seasonal difference.

#### 3.3.2. Remote Sensing Greenhouse Gases Observations

From a remote-sensing point of view, total columns of $CO_2$, CO, and $CH_4$ were measured for the first time in Thessaloniki, Greece, using a portable direct-solar viewing FTIR spectrometer since 2020, as part of the COllaborative Carbon Column Observing Network (COCCON [22]), with the goal of contributing to the validation of space-borne sensors and of detecting local sources of GHG in the future. Both $CH_4$ and $CO_2$ FTIR measurements were compared with the high spatial-resolution TROPOspheric Monitoring Instrument (TROPOMI). The $XCO_2$ remote-sensing timeseries (Figure 9a) also shows a discernible seasonal cycle with a winter and spring maximum driven by anthropogenic emissions, similar to in situ data, and a summer minimum due to biospheric activity at a typical mid-latitude Northern Hemisphere location. The biospheric signal could also contribute to the winter/spring maximum of $CO_2$, but in urban areas such as Athens and Thessaloniki, the green areas are significantly lacking; therefore, such signals should be masked by the

predominant anthropogenic sources. The $XCO_2$ timeseries also reveals higher winter and lower summer levels reflecting the common sources with $CO_2$, albeit with a large daily variability due to local influences and fire episodes. Concerning $XCH_4$, a rise begins in the summer (Figure 9b), when maximum temperatures occur, to reach its maximum levels in the wintertime, when most anthropogenic emissions occur. Compared to TROPOMI measurements (Figure 9c), $CH_4$ observations verify that the satellite data are within the official product requirements with a relative mean bias of $0.1 \pm 0.5\%$ [42]. TROPOMI captures the temporal $XCH_4$ variability, both the seasonal cycle with the profound summer growth as well as the overall higher values from year to year. TROPOMI also reproduces the $XCH_4$ enhancements from the fire episodes during July 2021 and August 2023 with a higher standard deviation (Figure 9b). The percentage variability of daily mean values in the course of the year was found to be ~2.9% in the case of $XCO_2$, while for $XCH_4$, it was found to be similar, at 3.7%. This translates to a 2.74 ppm annual mean difference in $XCO_2$ levels and a 15 ppb annual mean difference for $XCH_4$, values comparable to those derived from the in situ measurements at Finokalia and HAC Observatories. These results were comparable to those obtained from previous studies of greenhouse gases, revealing the biospheric cycle for $CO_2$ and relatively stable sources for $CH_4$ [24].

The $CO_2$ column concentrations retrieved from the OCO-2 observations in 2019 [42] and 2022 are presented for four different months of the two years, representing the four seasons of periods before and after COVID-19 (Figure 10). In order to indicate the location of hotspot sources, the tropospheric $NO_2$ column from S5P-TROPOMI observations re-gridded in a $0.2^\circ \times 0.2^\circ$ grid is shown as background in the same figure to indicate hotspot sources. Missing data have not been considered during the re-gridding procedure. The $CO_2$ column observations from OCO-2 capture reasonably well the seasonal variability of the observed $CO_2$ levels at Finokalia observatory, with high winter and low summer levels. In the same figure, the tropospheric $NO_2$ column distribution from TROPOMI 5p clearly shows the pollution produced from megacities, large agglomerations, and ships. However, the scarcity of OCO-2 observations (small swath width of 10 km and spatial resolution of 3 $km^2$), compared to TROPOMI $NO_2$ columns (swath width of about 2600 km and spatial resolution of $7 \times 3.5$ $km^2$), requires the combination of the two satellite products together with ground-based measurements and numerical modeling to geo-locate, monitor, and mitigate $CO_2$ emission sources.

Methane column concentrations have also been systematically studied over Greece, derived from the Sentinel-5 Precursor TROPOMI satellite instrument L-2 (high spatial resolution) data for the period 2019–2020. The data were first re-gridded into $0.2^\circ \times 0.2^\circ$ grids, and an increase in $CH_4$ columns was found between 2019 and 2020 (Figure 11) [43]. We identify Athens, Thessaly (central Greece), Thessaloniki (Northern Greece), Thrace (Northeastern Greece), and Crete (Southern Greece) as areas with high $CH_4$ concentrations due to the different anthropogenic activities in the area (Figure 11). Areas with biogas units, municipal waste disposal and treatment (e.g., Athens and Thessaloniki), and agricultural fields (e.g., Thessaly, Thrace, and Crete) are expected to have higher concentrations. An overall rise in $CH_4$ concentrations is observed in 2020 compared to 2019, following the global trends in $CH_4$, while an overall growth of about 8% has been observed in 2022 since 2003 [44]. This increase is as high as 12 ppb over Athens, which is in the same order of the one observed from the in situ data (15.8 ppb) and 22 ppb over Thessaloniki compared to the annual value of 15.20 ppb in globally averaged atmospheric $CH_4$ reported by NOAA in 2020 for marine sites [6].

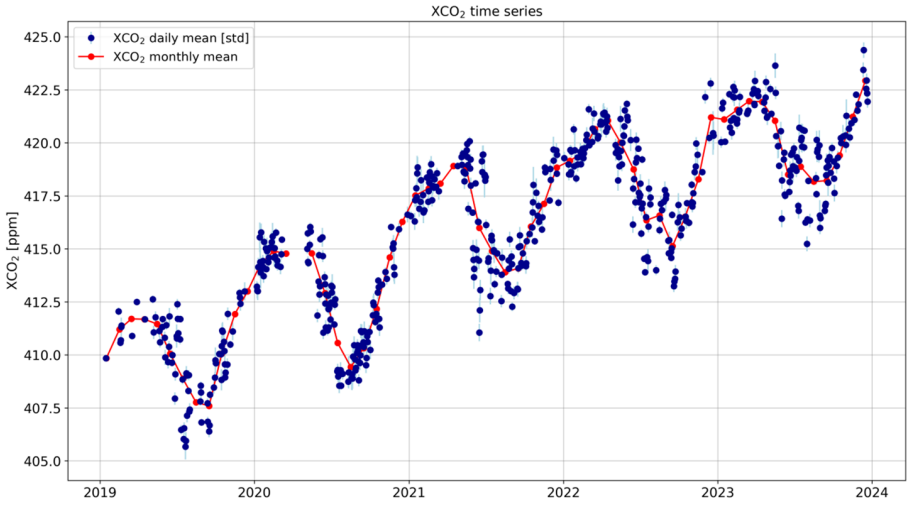


(**a**)

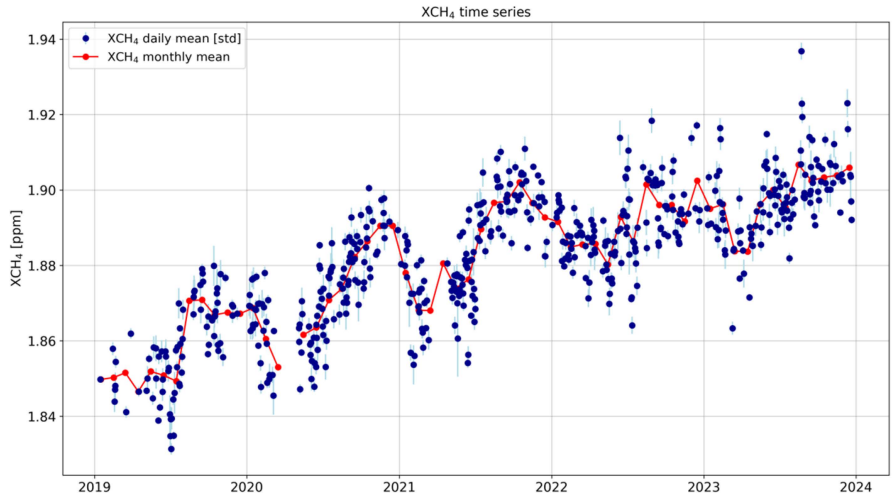


(**b**)

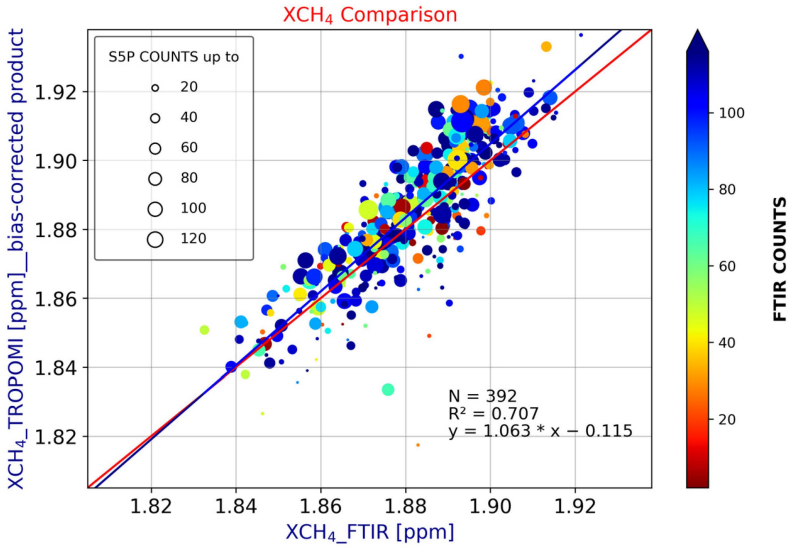


(**c**)

**Figure 9.** Dry air mole fraction of $CO_2$ (**a**) and $CH_4$ (**b**) over Thessaloniki from March 2019 to December 2023. The daily mean and associated standard deviation are in blue dots, and monthly means are in red dots. (**c**) Scatter plot between S5P/TROPOMI and FTIR observations for $CH_4$ (**c**) over Thessaloniki for the same period.

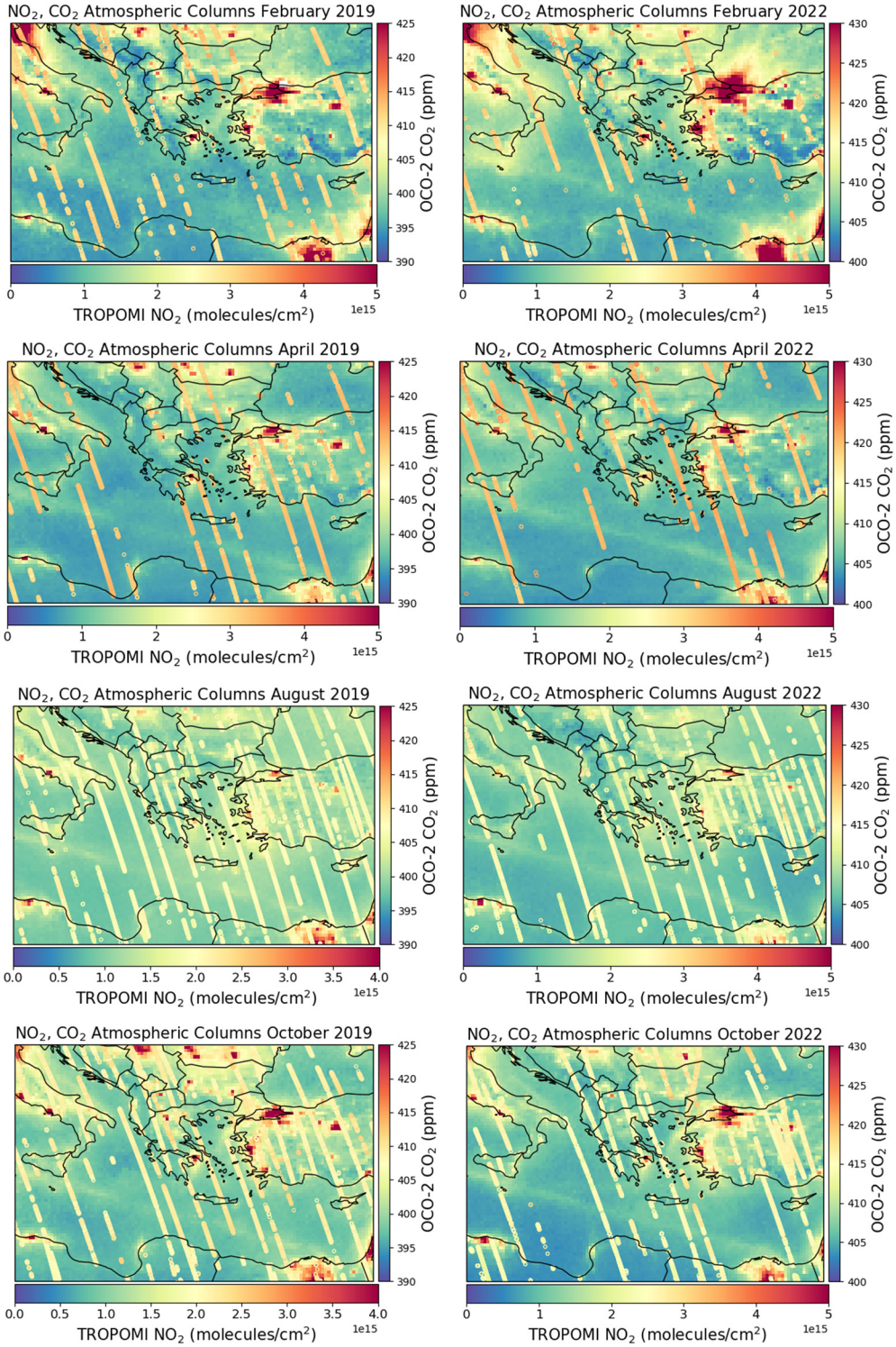


**Figure 10.** Monthly mean tropospheric $NO_2$ column data from TROPOMI (map) and $CO_2$ column concentrations from OCO-2 (circles in strip lines) for February, April, October, and August of 2019 (**left** panels) and of 2022 (**right** panels) over the eastern Mediterranean. Figures for 2019 from [42].

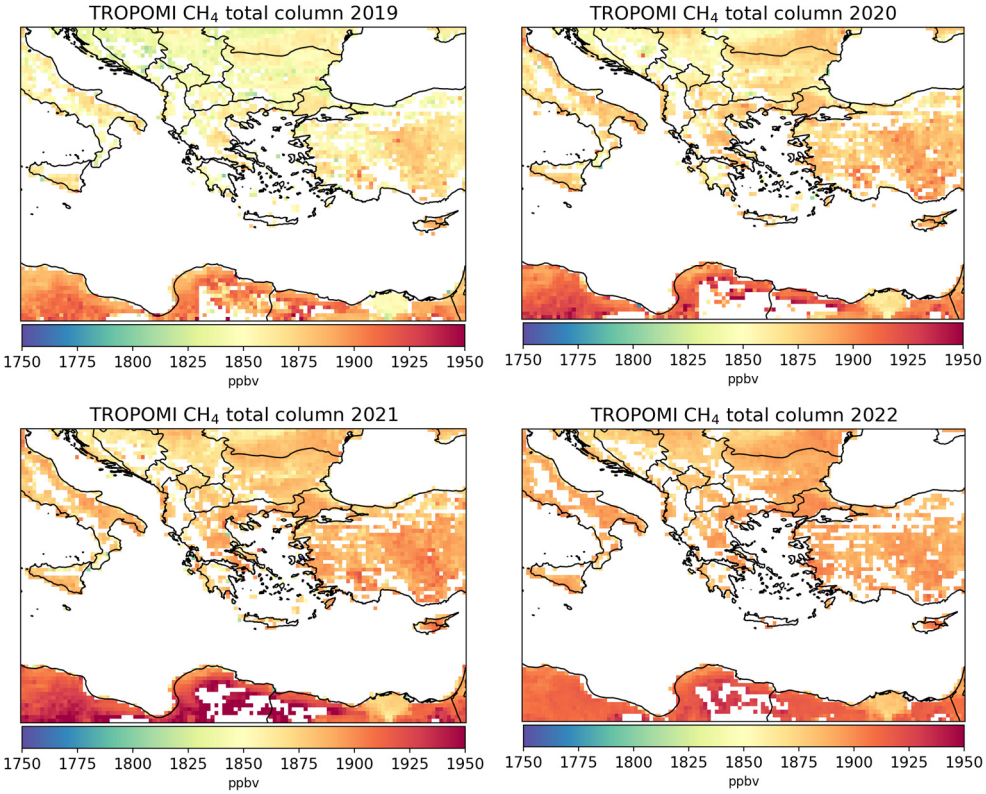


**Figure 11.** Annual mean TROPOMI $CH_4$ column distribution for 2019, 2020, 2021, and 2022. Figures for 2019 and 2020 are from [42].

### *3.4. Greenhouse Gas Levels and Global Pandemic*

In the first few years after the COVID-19 global pandemic, it would be expected that GHG levels would decrease due to the overall restrictive measures. Le Quéré et al. [45] estimated a 27% reduction in average daily $CO_2$ emissions in Greece in 2020, within the range of reductions in EU countries reported in the same study, due to reduced mobility and production during the lockdown period. Similarly, a 20% reduction on the mean carbon footprint during the lockdown period has been estimated for Italy, mostly affecting the northern industrialized areas of the country [46]. For the entire year of 2020 European emissions, the second largest reduction attributed to the COVID-19 lockdown measures was for $CO_2$ fossil fuel (−7.8%) [47]. For neighboring Türkiye, the decline in the global warming potential for April and May 2020 was on average 10, 38, and 36% for diesel, gasoline, and liquefied petroleum gas fuel, respectively [48]. Average $CO_2$ levels in Athens declined by 2.1% (9.1 ppm) during the lockdown compared to the pre-lockdown period, a change that, although subtle, is still statistically significant at the 99% confidence level ($p < 0.01$) [49]. After subtracting the respective average regional background concentrations from Finokalia for the same period, the resulting amount is considered the "excess" amount of $CO_2$ for Athens; therefore, the relative reduction in $CO_2$ during the lockdown period was 58%, comparable to those observed in major cities internationally [50]. The large reduction observed in Athens should also be attributed, in addition to reduced mobility, to the significant effect of additional sources [51,52] related to the seasonal cycle of residential heating (wood-burning and also the combustion of heating oil and natural gas), which—independent of the lockdown measures—dropped until the end of the heating season in Athens (mid-April) [41]. Nevertheless, this localized reduction was not reflected in the global average level of $CO_2$, which reached a new record high of 412.5 ppm in 2020. Surprisingly, while $CO_2$ emissions fell by 5.4% in 2020, the amount of $CO_2$ in the atmosphere continued to grow at about the same rate as in previous years. Estimates of how much $CH_4$ emissions dropped during the pandemic are uncertain because some human

causes, such as poor maintenance of oilfield infrastructure, are not well documented, but one study calculated that the reduction was 10% [53]. In Athens, average $CH_4$ levels were reduced by 0.5% (10 ppb) during the lockdown period compared to the pre-lockdown period. After subtracting the respective period-averaged regional background concentration from Finokalia, the reduction in $CH_4$ during the lockdown was 15%. This small difference compared to $CO_2$ may be due to people spending more time inside their houses and not reducing their waste production and energy use. Despite the dramatic decline in mobility and associated vehicle emissions, the atmospheric growth rates of GHG were not slowed, in part due to reduced ocean uptake of $CO_2$ and a likely increase in $CH_4$ lifetime from reduced $NO_x$ emissions [53], leading to new global average records for $CO_2$ in 2020 and $CH_4$ in 2021.

## 4. Conclusions

This study presents an overview of greenhouse gas sources, levels, and trends over Greece, with an emphasis on $CO_2$ and $CH_4$. In Greece, more than 90% of the $CO_2$ is produced by fossil fuel consumption, followed by transport and construction. Moreover, waste management is the main anthropogenic source of $CH_4$, accounting for 47% of total emissions and surpassing emissions from agriculture since 2017.

GHG levels systematic monitoring in Greece started at the remote background site of Finokalia Observatory in Crete, with a twenty-year record of measurements showing an increase in $CO_2$ by 2.4 ppm·yr$^{-1}$ between 2002 and 2023, following the average rate of rise in $CO_2$ in the north hemisphere. The same increasing rate is also derived from free tropospheric measurements at the Helmos Observatory since 2016. These background sites exhibit spring maxima and summer minima, while the urban background site in Athens shows a distinct winter maximum attributed to the additional anthropogenic emissions for heating purposes. On the one hand, levels in Athens during summer are the lowest, reaching levels similar to those observed for the other two background sites, indicating that during late spring and summer, the relative contribution of $CO_2$ sources and sinks is markedly different, with significant contribution from regional rather than local sources. On the other hand, during autumn and especially during winter, local sources, mainly heating and traffic, are the main contributors of $CO_2$ levels in Athens. $CH_4$ levels also show an increasing trend in Greece, with 8.6 ppb·yr$^{-1}$ at Finokalia since 2002 but at an accelerated rate since 2018 (13.1 ppb·yr$^{-1}$), also seen at the HAC Observatory, possibly associated with a combination of local and regional sources. For the common period of measurements (2018–2023), $CH_4$ showed comparable growth at all three sites (~14 ppb·yr$^{-1}$).

The increase seen by the in situ observations is also corroborated by the remote sensing data of GHG performed in Thessaloniki. The remote-sensing timeseries also shows a clear seasonal cycle with a winter and spring maximum attributed to enhanced anthropogenic sources and a summer minimum. The TROPOMI data are also used to identify areas with elevated levels, such as Athens, Thessaly, Thessaloniki, and Thrace, due to different anthropogenic activities.

Finally, comparison of observations before and after the COVID-19 global pandemic enabled the identification of the impact of restriction measures on GHG levels. Average $CO_2$ levels in Athens decreased by 2.1% (9.1 ppm) during the lockdown compared to the pre-lockdown period, but when subtracting the respective period average concentrations from the remote background measured at the Finokalia site, the actual reduction in $CO_2$ was 58%, comparable to those observed in major cities globally. The respective reduction in $CH_4$ after subtracting the background signal was of the order of 15% since the emission sources differ from those mostly affected by the implemented restrictions. Nevertheless, the restriction measures and their effects may provide insight into possible mitigation strategies in order to attain the European Green Deal goals.

**Author Contributions:** Conceptualization, A.B., M.K. and N.M.; methodology, N.G., Y.S., M.I.G., M.M., S.M. and M.K.; software, S.M., N.G., M.I.G. and M.M.; validation, A.B., N.G., C.N., M.I.G. and M.M.; formal analysis, A.B., N.G. and C.N.; resources, D.B., K.E., M.K. and N.M.; data curation,

A.B., P.K., N.G., C.N., M.L., M.I.G. and M.M.; writing—original draft preparation, A.B. and N.M.; writing—review and editing, Y.S., M.R., C.N., S.M. and M.K.; visualization, A.B., P.K., N.G., M.I.G. and M.M.; supervision, D.B., K.E., M.R., M.K. and N.M.; project administration, K.E., M.K. and N.M.; funding acquisition, N.M. All authors have read and agreed to the published version of the manuscript.

**Funding:** This research was funded by the project "Support for Enhancing the Operation of the National Network for Climate Change (CLIMPACT)" of the National Development Program, by the General Secretariat of Research and Innovation, Greece (2023NA11900001—N. 5201588).

**Institutional Review Board Statement:** Not applicable.

**Informed Consent Statement:** Not applicable.

**Data Availability Statement:** The raw data supporting the conclusions of this article will be made available by the authors on request. COCCON Version 1 dataset from atmospheric observatory of Thessaloniki available at the EVDC Data Handling Facilities, https://doi.org/10.48477/coccon.pf10.thessaloniki.R01, COCCON-Central Facility/EVDC-ESA Atmospheric Validation Data Centre.

**Acknowledgments:** N.G. and M.K. acknowledge the Deutsche Forschungsgemeinschaft (DFG, German Research Foundation) under Germany's Excellence Strategy (University Allowance, EXC 2077, University of Bremen) and the HORIZON-WIDERA, grant no. 101071247 EDU4CLIMATE.

**Conflicts of Interest:** The authors declare no conflicts of interest.

## References

1. *IPCC Climate Change 2022. The Physical Science Basis. Summary for Policymakers*; IPCC: Cambridge, UK; New York, NY, USA, 2022.
2. Global Monitoring Laboratory. Trends in Atmospheric Carbon Dioxide ($CO_2$). Available online: https://gml.noaa.gov/ccgg/trends/ (accessed on 8 August 2024).
3. Lindsey, R. Climate Change: Atmospheric Carbon Dioxide. Available online: https://www.climate.gov/news-features/understanding-climate/climate-change-atmospheric-carbon-dioxide (accessed on 14 August 2024).
4. Friedlingstein, P.; O'Sullivan, M.; Jones, M.W.; Andrew, R.M.; Bakker, D.C.E.; Al, E. Global Carbon Budget 2023. *Earth Syst. Sci. Data* **2023**, *15*, 5301–5369. [CrossRef]
5. Saunois, M.; Martinez, A.; Poulter, B.; Zhang, Z.; Raymond, P.A.; Canadell, J.G.; Jackson, R.B.; Patra, P.K.; Bousquet, P. Global Methane Budget 2000–2020. *Earth Syst. Sci. Data Discuss (preprint)* **2024**. [CrossRef]
6. Global Monitoring Laboratory. Trends in Atmospheric Methane ($CH_4$). Available online: https://gml.noaa.gov/ccgg/trends_ch4/ (accessed on 12 August 2024).
7. Voulgarakis, A.; Naik, V.; Lamarque, J.-F.; Shindell, D.T.; Young, P.J.; Prather, M.J.; Wild, O.; Field, R.D.; Bergmann, D.; Cameron-Smith, P.; et al. Analysis of Present Day and Future OH and Methane Lifetime in the ACCMIP Simulations. *Atmos. Chem. Phys.* **2013**, *13*, 2563–2587. [CrossRef]
8. Jackson, R.B.; Saunois, M.; Bousquet, P.; Canadell, J.G.; Poulter, B.; Stavert, A.R.; Bergamaschi, P.; Niwa, Y.; Segers, A.; Tsuruta, A. Increasing Anthropogenic Methane Emissions Arise Equally from Agricultural and Fossil Fuel Sources. *Environ. Res. Lett.* **2020**, *15*, 071002. [CrossRef]
9. European Union and the United States Global Methane Pledge. Available online: https://www.globalmethanepledge.org/ (accessed on 26 May 2024).
10. Gialesakis, N.; Kalivitis, N.; Kouvarakis, G.; Ramonet, M.; Lopez, M.; Kwok, C.Y.; Narbaud, C.; Daskalakis, N.; Mermigkas, M.; Mihalopoulos, N.; et al. A Twenty Year Record of Greenhouse Gases in the Eastern Mediterranean Atmosphere. *Sci. Total Environ.* **2023**, *864*, 161003. [CrossRef]
11. Papadimas, C.D.; Hatzianastassiou, N.; Mihalopoulos, N.; Kanakidou, M.; Katsoulis, B.D.; Vardavas, I. Assessment of the MODIS Collections C005 and C004 Aerosol Optical Depth Products over the Mediterranean Basin. *Atmos. Chem. Phys.* **2009**, *9*, 2987–2999. [CrossRef]
12. Levieveld, J.; Berresheim, H.; Bormann, S.; Crutzen, P.J.; Dentener, F.J.; Fischer, H.; Feichter, J.; Flatau, P.J.; Heland, J.; Holzinger, R.; et al. Global Air Pollution Crossroads over the Mediterranean. *Science* **2002**, *298*, 794–799. [CrossRef]
13. Zittis, G.; Almazroui, M.; Alpert, P.; Ciais, P.; Cramer, W.; Dahdal, Y.; Fnais, M. Climate Change and Weather Extremes in the Eastern Mediterranean and Middle East. *Rev. Geophys.* **2022**, *60*, e2021RG000762. [CrossRef]
14. Urdiales-Flores, D.; Zittis, G.; Hadjinicolaou, P.; Osipov, S.; Klingmüller, K.; Mihalopoulos, N.; Kanakidou, M.; Economou, T.; Lelieveld, J. Drivers of Accelerated Warming in Mediterranean Climate-Type Regions. *NPJ Clim. Atmos. Sci.* **2023**, *6*, 97. [CrossRef]
15. IPCC 2006 IPCC Guidelines for National Greenhouse Gas Inventories, Prepared by the National Greenhouse Gas Inventories Programme. Available online: https://www.ipcc-nggip.iges.or.jp/public/2006gl/ (accessed on 17 April 2024).
16. Picarro Datasheet GasScouter G2401 $CO_2$, CO, $CH_4$ and $H_2O$ Analyzer. Available online: https://www.picarro.com/support/library/documents/g2401_analyzer_datasheet (accessed on 22 February 2024).

17. Dimitriou, K.; Bougiatioti, A.; Ramonet, M.; Pierros, F.; Michalopoulos, P.; Liakakou, E.; Solomos, S.; Quehe, P.Y.; Delmotte, M.; Gerasopoulos, E.; et al. Greenhouse Gases ($CO_2$ and $CH_4$) at an Urban Background Site in Athens, Greece: Levels, Sources and Impact of Atmospheric Circulation. *Atmos. Environ.* **2021**, *253*, 118372. [CrossRef]
18. ICOS RI ICOS Atmosphere Station Specifications V2.0. ICOS ERIC. Available online: https://doi.org/10.18160/GK28-2188 (accessed on 26 May 2024). [CrossRef]
19. Yver-Kwok, C.; Philippon, C.; Bergamaschi, P.; Biermann, T.; Calzolari, F.; Chen, H.; Conil, S.; Cristofanelli, P.; Delmotte, M.; Hatakka, J.; et al. Evaluation and Optimization of ICOS Atmosphere Station Data as Part of the Labeling Process. *Atmos. Meas. Tech.* **2021**, *14*, 89–116. [CrossRef]
20. Kouvarakis, G.; Vrekoussis, M.; Mihalopoulos, N.; Kourtidis, K.; Rappenglueck, B.; Gerasopoulos, E.; Zerefos, C. Spatial and Temporal Variability of Tropospheric Ozone ($O_3$) in the Boundary Layer above the Aegean Sea (Eastern Mediterranean). *J. Geophys. Res. Atmos.* **2002**, *107*, PAU 4-1–PAU 4-14. [CrossRef]
21. Kalivitis, N.; Gerasopoulos, E.; Vrekoussis, M.; Kouvarakis, G.; Kubilay, N.; Hatzianastassiou, N.; Vardavas, I.; Mihalopoulos, N. Dust Transport over the Eastern Mediterranean Derived from Total Ozone Mapping Spectrometer, Aerosol Robotic Network, and Surface Measurements. *J. Geophys. Res. Atmos.* **2007**, *112*, D03202. [CrossRef]
22. Frey, M.; Sha, M.K.; Hase, F.; Kiel, M.; Blumenstock, T.; Harig, R.; Surawicz, G.; Deutscher, N.M.; Shiomi, K.; Franklin, J.E.; et al. Building the COllaborative Carbon Column Observing Network (COCCON): Long-Term Stability and Ensemble Performance of the EM27/SUN Fourier Transform Spectrometer. *Atmos. Meas. Tech.* **2019**, *12*, 1513–1530. [CrossRef]
23. Gisi, M.; Hase, F.; Dohe, S.; Blumenstock, T.; Simon, A.; Keens, A. $XCO_2$-Measurements with a Tabletop FTS Using Solar Absorption Spectroscopy. *Atmos. Meas. Tech.* **2012**, *5*, 2969–2980. [CrossRef]
24. Mermigkas, M.; Topaloglou, C.; Balis, D.; Koukouli, M.E.; Hase, F.; Dubravica, D.; Borsdorff, T.; Lorente, A. Ftir Measurements of Greenhouse Gases over Thessaloniki, Greece in the Framework of Coccon and Comparison with S5p/Tropomi Observations. *Remote Sens.* **2021**, *13*, 3395. [CrossRef]
25. Global Monitoring Laboratory. NOAA/GML Calculation of Global Means. Available online: https://gml.noaa.gov/ccgg/about/global_means.html (accessed on 14 August 2024).
26. Ministry of Environment and Energy (MEEN). *National Inventory Report of Greece for Greenhouse and Other Gases for the Years 1990–2021*; Ministry of Environment and Energy (MEEN), Greece: Athens, Greece, 2023. Available online: https://ypen.gov.gr/wp-content/uploads/2024/04/2024_NIR_Greece.pdf (accessed on 14 August 2024).
27. EEA Trends and Projections in Europe 2023. 2023. Available online: https://www.eea.europa.eu/publications/trends-and-projections-in-europe-2023 (accessed on 14 August 2024).
28. Lalas, D.; Gakis, N.; Mirasgedis, S.; Georgopoulou, E.; Sarafidis, Y.; Doukas, H. Energy and GHG Emissions Aspects of the COVID Impact in Greece. *Energies* **2021**, *14*, 1955. [CrossRef]
29. United Nations Climate Change National Inventory Submissions. 2023. Available online: https://unfccc.int/ghg-inventories-annex-i-parties/2023 (accessed on 16 October 2024).
30. Bange, H.W.; Rapsomanikis, S.; Andreae, M.O. The Aegean Sea as a Source of Atmospheric Nitrous Oxide and Methane. *Mar. Chem.* **1996**, *53*, 41–49. [CrossRef]
31. Blanco, G.R.; Gerlagh, S.; Suh, J.; Barrett, H.C.; de Coninck, C.F.; Diaz Morejon, R.; Mathur, N.; Nakicenovic, A.; Ofosu Ahenkora, J.; Pan, H.; et al. Drivers, Trends and Mitigation. In *Climate Change 2014: Mitigation of Climate Change. Contribution of Working Group III to the Fifth Assessment Report of the Intergovernmental Panel on Climate Change*; Cambridge University Press: New York, NY, USA, 2014. Available online: https://www.ipcc.ch/site/assets/uploads/2018/02/ipcc_wg3_ar5_full.pdf (accessed on 14 August 2024).
32. Hoekstra, R.; Bergh, J.J.C.J.M. Van Der Comparing Structural and Index Decomposition Analysis. *Energy Econ.* **2003**, *25*, 39–64. [CrossRef]
33. European Commission's Directorate General for Economic and Financial Affairs AMECO. Available online: https://ec.europa.eu/info/business-economy-euro/indicators-statistics/economic-databases/macro-economic-database-ameco/ameco-database_en (accessed on 22 February 2024).
34. European Commission SHARES Tool. Available online: https://ec.europa.eu/eurostat/documents/38154/4956088/SHARES-2013-manual.pdf (accessed on 22 February 2024).
35. Coen, M.C.; Andrews, E.; Aliaga, D.; Andrade, M.; Angelov, H. Identification of Topographic Features Influencing Aerosol Observations at High Altitude Stations. *Atmos. Chem. Phys.* **2018**, *18*, 12289–12313. [CrossRef]
36. Zografou, O.; Gini, M.; Fetfatzis, P.; Granakis, K.; Foskinis, R. High-Altitude Aerosol Chemical Characterization and Source Identification: Insights from the CALISHTO Campaign. *Atmos. Chem. Phys.* **2024**, *24*, 8911–8926. [CrossRef]
37. Azoukis, S.; Akamati, K.; Bizelis, I.; Laliotis, G.P. Retrospective Assessment of Greenhouse Gas Emissions from the Beef Sector in Greece and Potential Mitigation Scenarios. *Environments* **2023**, *10*, 144. [CrossRef]
38. Dlugokencky, E.J.; Lang, P.M.; Masade, K.A. The Growth Rate and Distribution of Atmospheric Methane. *J. Geophys. Res.* **1994**, *99*, 17021–17043.
39. Zhang, M.; Zhang, X.-Y.; Liu, R.-X.; Hu, L.-Q. A Study of the Validation of Atmospheric $CO_2$ from Satellite Hyper Spectral Remote Sensing. *Adv. Clim. Chang. Res.* **2014**, *5*, 131–135. [CrossRef]

40. Dimitriou, K.; Stavroulas, I.; Grivas, G.; Chatzidiakos, C.; Kosmopoulos, G.; Kazantzidis, A.; Kourtidis, K.; Karagioras, A.; Hatzianastassiou, N.; Pandis, S.; et al. Intra- and Inter-City Variability of PM2.5 Concentrations in Greece as Determined with a Low-Cost Sensor Network. *Atmos. Environ.* **2023**, *301*, 119713. [CrossRef]
41. Liakakou, E.; Stavroulas, I.; Kaskaoutis, D.G.; Grivas, G.; Paraskevopoulou, D.; Dumka, U.C.; Tsagkaraki, M.; Bougiatioti, A.; Oikonomou, K.; Sciare, J.; et al. Long-Term Variability, Source Apportionment and Spectral Properties of Black Carbon at an Urban Background Site in Athens, Greece. *Atmos. Environ.* **2020**, *222*, 117137. [CrossRef]
42. Koukouli, M.E.; Skoulidou, I.; Karavias, A.; Parcharidis, I.; Balis, D.; Manders, A.; Segers, A.; Eskes, H.; Van Geffen, J. Sudden Changes in Nitrogen Dioxide Emissions over Greece Due to Lockdown after the Outbreak of COVID-19. *Atmos. Chem. Phys.* **2021**, *21*, 1759–1774. [CrossRef]
43. Evangelou, I.; Gialesakis, N.; Daskalakis, N.; Kanakidou, M. Methane Distribution over Greece as Derived from Sentinel-5P TROPOMI Data. *CEST 2021* **2021**, CEST2021_00758.
44. Kourtidis, K.; Tzivleris, A.; Stathopoulos, S.; Gemitzi, A.; Georgoulias, A.K. On the Methane Emissions of the Greater Thessaloniki Area. *Environ. Sci. Proc.* **2023**, *26*, 39. [CrossRef]
45. Quéré, C.L.; Jackson, R.B.; Jones, M.W.; Smith, A.J.P.; Abernethy, S.; Andrew, R.M.; De-gol, A.J.; Willis, D.R.; Shan, Y.; Canadell, J.G.; et al. During the COVID-19 Forced Confinement. *Nat. Clim. Chang.* **2020**, *10*, 647–654. [CrossRef]
46. Rugani, B.; Caro, D. Impact of COVID-19 Outbreak Measures of Lockdown on the Italian Carbon Footprint. *Sci. Total Environ.* **2020**, *737*, 139806. [CrossRef] [PubMed]
47. Guevara, M.; Petetin, H.; Jorba, O.; Denier Van Der Gon, H.; Kuenen, J.; Super, I.; Jalkanen, J.P.; Majamaki, E.; Johansson, L.; Peuch, V.H.; et al. European Primary Emissions of Criteria Pollutants and Greenhouse Gases in 2020 Modulated by the COVID-19 Pandemic Disruptions. *Earth Syst. Sci. Data* **2022**, *14*, 2521–2552. [CrossRef]
48. Gürbüz, H.; Şöhret, Y.; Ekici, S. Evaluating Effects of the COVID-19 Pandemic Period on Energy Consumption and Enviro-Economic Indicators of Turkish Road Transportation. *Energy Sources Part A Recover. Util. Environ. Eff.* **2021**, 1–13. [CrossRef]
49. Grivas, G.; Athanasopoulou, E.; Kakouri, A.; Bailey, J.; Liakakou, E.; Stavroulas, I.; Kalkavouras, P.; Bougiatioti, A.; Kaskaoutis, D.G.; Ramonet, M.; et al. Integrating in Situ Measurements and City Scale Modelling to Assess the COVID–19 Lockdown Effects on Emissions and Air Quality in Athens, Greece. *Atmosphere* **2020**, *11*, 1174. [CrossRef]
50. Nicolini, G.; Antoniella, G.; Carotenuto, F.; Christen, A.; Ciais, P.; Feigenwinter, C.; Gioli, B.; Stagakis, S.; Velasco, E.; Vogt, R.; et al. Direct Observations of $CO_2$ Emission Reductions Due to COVID-19 Lockdown across European Urban Districts. *Sci. Total Environ.* **2022**, *830*, 154662. [CrossRef]
51. Stagakis, S.; Chrysoulakis, N.; Spyridakis, N.; Feigenwinter, C.; Vogt, R. Eddy Covariance Measurements and Source Partitioning of $CO_2$ Emissions in an Urban Environment: Application for Heraklion, Greece. *Atmos. Environ.* **2019**, *201*, 278–292. [CrossRef]
52. Gioli, B.; Toscano, P.; Lugato, E.; Matese, A.; Miglietta, F.; Zaldei, A.; Vaccari, F.P. Methane and Carbon Dioxide Fl Uxes and Source Partitioning in Urban Areas: The Case Study of Florence, Italy. *Environ. Pollut.* **2012**, *164*, 125–131. [CrossRef]
53. Laughner, J.L.; Neu, J.L.; Schimel, D.; Wennberg, P.O.; Barsanti, K.; Bowman, K.W.; Chatterjee, A.; Croes, B.E.; Fitzmaurice, H.L.; Henze, D.K.; et al. Societal Shifts Due to COVID-19 Reveal Large-Scale Complexities and Feedbacks between Atmospheric Chemistry and Climate Change. *Proc. Natl. Acad. Sci. USA* **2021**, *118*, e2109481118. [CrossRef]